Research Square

Preprints are preliminary reports that have not undergone peer review.
They should not be considered conclusive, used to inform clinical practice,
or referenced by the media as validated information.

Interpreting elemental signatures at palm-leaf manuscript inscriptions through historical and experimental evidence using synchrotron XRF

Laura Gallardo

laura.gallardo@tuhh.de

Hamburg University of Technology

Mark Busch

Hamburg University of Technology

Giovanni Ciotti

University of Bologna

Patrick Huber

Hamburg University of Technology

Article

Keywords: Palm-leaf manuscripts, multimodal analysis, SAXS, WAXS, XRF, synchrotron radiation, non-destructive analysis, archaeometry, cultural heritage, inscriptions, ink

Posted Date: November 6th, 2026

DOI: https://doi.org/10.21203/rs.3.rs-11626625/v1

License: This work is licensed under a Creative Commons Attribution 4.0 International License.
Read Full License

Additional Declarations: No competing interests reported.

Interpreting synchrotron XRF elemental signatures at palm-leaf manuscript inscriptions through historical and experimental evidence

Laura Gallardo*[1], Mark Busch[1,2], Giovanni Ciotti[3,4], and Patrick Huber[1,2]

[1]Hamburg University of Technology, Institute for Materials and X-ray Physics, Hamburg, Germany
[2]Centre for X-ray and Nano Science CXNS, Deutsches Elektronen-Synchrotron DESY, Hamburg, Germany
[3]Centre for the Study of Manuscript Cultures CSMC, Universität Hamburg, Warburgstraße 26, 20354, Hamburg, Germany
[4]Department of History and Cultures, University of Bologna, Bologna, Italy

November 4, 2026

Abstract

Palm-leaf manuscript traditions are diverse, but many employ a common writing procedure: text is incised with a stylus and subsequently made visible by rubbing dark material into the grooves. Elevated metal signals have been reported at such inscriptions, although their origin remains uncertain. Here, synchrotron X-ray fluorescence mapping was applied to the palm-leaf manuscript collection of the Centre for the Study of Manuscript Cultures CSMC (Hamburg) and to experimental mock-ups to examine possible contributions from stylus abrasion, blackening materials, and preservation treatments. Historical manuscripts showed that these contributions may coexist. Similar elemental enrichment at inscriptions and cracks suggests an important contribution from applied materials accumulating in surface discontinuities. Conversely, apparently unblackened inscriptions retained localized metal enrichment, consistent with a contribution associated with incision. Comparisons with binding holes and edges, which are also tool-produced features, further supported a multifactorial origin. The mock-ups did not show consistently detectable enrichment from stylus use alone. However, traditionally used materials produced localized effects: neem oil increased Fe signals, and burnt candlenut increased Mn signals. Elemental signatures therefore record complex material histories including tool-derived and applied material contributions.

Keywords: Palm-leaf manuscripts, multimodal analysis, SAXS, WAXS, XRF, synchrotron radiation, non-destructive analysis, archaeometry, cultural heritage, inscriptions, ink

Introduction

Palm-leaf manuscripts have served as writing supports for centuries across South and Southeast Asia. They remain important cultural and religious objects and, in some regions, continue to be produced in workshops that maintain or revive local knowledge and craft practices. The preparation of palm leaves, their inscription, and their subsequent treatment vary substantially

*Corresponding author: laura.gallardo@tuhh.de

between regions and traditions [1, 2], reflecting both the long history and the wide geographical distribution of palm-leaf manuscript cultures.

Two principal writing techniques are used on palm leaves. Text may be written directly on the surface with a pen or brush, or it may be incised with a stylus. In the latter technique, widespread in South India, Sri Lanka, and parts of Southeast Asia, the incisions are made visible by rubbing a dark material over the leaf and removing the excess from the surface. The remaining material is retained preferentially within the grooves [1]. Blackening mixtures commonly contain soot or lampblack combined with an oil or other binding medium; in some Indonesian traditions, burnt candlenut is rubbed directly over the surface [3]. The same leaves may also receive oils or other substances during use and preservation, adding further material to the manuscript surface [4, 5].

Recent analytical studies have begun to characterize these writing materials directly. Non-invasive microscopy, FTIR spectroscopy, and XRF distinguished incised manuscripts from Yunnan, in which black material was retained in the grooves, from liquid-ink palm-leaf manuscripts of South Asian origin preserved in Tibet, which showed different ink compositions and degradation behaviour [6]. A subsequent multi-analytical study of a Tibetan palm-leaf manuscript identified lamp soot derived from oil combustion and indicated the presence of adhesive components, including animal glue and plant gum [7]. Material characterization of nineteenth- and twentieth-century manuscripts from Northern Thailand likewise confirmed the use of carbon-based material in incised writing, and trace Fe was detected in one manuscript. Stylus abrasion was mentioned as a possible Fe contribution [8]. Studies of Indian palm-leaf manuscripts further demonstrate that both organic binders and a broad range of mineral and plant-derived colourants may occur in manuscript materials [4, 9].

These findings establish that the visible material at palm-leaf inscriptions is chemically complex and that its composition depends on both writing technique and local material practices. However, the origin of metallic signals detected specifically at incised lines remains poorly resolved. Previous XRF investigations, including our earlier measurements, have identified localized enhancement of transition-metal signals, especially Fe, at inscriptions [8, 10]. Such enrichment may arise through abrasion or transfer from a metallic stylus during incision. Yet metals may also be introduced by soot-based blackening mixtures, oils and other preservation media, contamination, or metal particles incorporated during the preparation and application of these materials. Consequently, an elemental signal at an inscription cannot automatically be interpreted as a stylus signature. Spatially resolved XRF has also been used to distinguish visually similar inks and reveal successive stages of writing, correction, and reinking in other manuscript traditions [11].

Synchrotron X-ray methods provide complementary information on the composition and structure of cultural heritage materials [12]. Here, we investigate the elemental composition of inscriptions in historical palm-leaf manuscripts from the CSMC collection using synchrotron X-ray fluorescence (XRF) mapping. Spatially resolved measurements allow inscriptional enrichment to be compared with that at other features, including binding holes, edges, and cracks, which have different manufacturing and material histories. Manuscripts with apparently unblackened inscriptions provide an additional opportunity to assess elemental signatures where visible blackening material is absent. To examine the relative contributions of incision and blackening, we additionally prepared and measured experimental mock-ups using traditional styluses and selected blackening procedures.

The study addresses three questions: which elements are enriched at historical inscriptions relative to their surrounding substrates; how do these enrichment patterns vary between objects and geographical groups; and to what extent can they be associated with stylus use, blackening procedures, or both. By combining historical manuscripts with experimental reconstructions, the study provides a framework for interpreting elemental enrichment at palm-leaf inscriptions as the result of intertwined writing, blackening, and preservation histories.

Methods

Mock-up preparation

Mock-ups were prepared using styluses of known composition and applying different coloring media to further investigate the elemental signatures observed at the inscriptions of historical manuscripts. Burnt candlenut is documented as a material used to make incised writing visible in Lombok [3]. Candlenut powder mixed with lemongrass oil is also documented in manuscript care practices in Surakarta [13], and Wiland lists additionally citronella, eucalyptus, and neem oils during preparation of the writing support or preservation treatments [5].

Leaves of both commonly used genera: *Borassus* and *Corypha* were tested, keeping control uninscribed writing support references. Traditional styluses from Thailand (lek chan) and from Indonesia (pengrupak) were selected to create the inscriptions. The former presents the appearance of a metallic pen-like object, while the latter resembles a knife, see the top panes in Fig. 7. Both were used by experienced practitioners to inscribe numbers and text on the reference writing support. Some of these inscriptions were left without blackening treatment to isolate possible material residues left by the stylus.

Glassware was used to prepare mixtures of soot and different oils and to apply them over the inscriptions, thereby ensuring no metal cross-contamination. Table 1 presents a list of the mock-up samples specifying genus, inscription, scribe, stylus and blackening treatment when applicable.

Table 1: Mock-up writing supports and inscription treatments investigated by XRF. Controls contained neither incisions nor applied blackening substances. Inscribed samples contain uncoloured inscriptions, i.e. they were incised but not subsequently blackened, and colored samples contain inscriptions and blackening material was applied. Detailed measurement identifiers and acquisition conditions are provided in Supplementary Data 1.

Mock-up ID	Condition	Inscription	Genus	Scribe	Stylus	Blackening treatment
thai-0-0-0-0	control	–	*Corypha*	–	–	–
ind-0-0-0-0	control	–	*Borassus*	–	–	–
thai-lc-0-text-L	inscribed	text	*Corypha*	Dr Jaengsawang	lek chan	–
ind-pg-0-text-C	inscribed	text	*Borassus*	Carma Citrawati	pengrupak	–
ind-pg-0-text-P	inscribed	text	*Borassus*	Istri Pebriyani	pengrupak	–
ind-lc-0-1-L	inscribed	1	*Borassus*	Dr Jaengsawang	lek chan	–
thai-lc-0-1-L	inscribed	1	*Corypha*	Dr Jaengsawang	lek chan	–
ind-pg-cn-text-P	colored	text	*Borassus*	Istri Pebriyani	pengrupak	Candlenut
thai-lc-sses-2-L	colored	2	*Corypha*	Dr Jaengsawang	lek chan	Sesame oil + soot
thai-lc-slem-3-L	colored	3	*Corypha*	Dr Jaengsawang	lek chan	Lemongrass oil + soot
thai-lc-snem-4-L	colored	4	*Corypha*	Dr Jaengsawang	lek chan	Neem oil + soot
thai-lc-sric-5-L	colored	5	*Corypha*	Dr Jaengsawang	lek chan	Castor oil + soot
thai-lc-scit-6-L	colored	6	*Corypha*	Dr Jaengsawang	lek chan	Citronella oil + soot
thai-lc-seuc-7-L	colored	7	*Corypha*	Dr Jaengsawang	lek chan	Eucalyptus oil + soot
thai-lc-slem-8-L	colored	8	*Corypha*	Dr Jaengsawang	lek chan	Lemongrass oil + soot
ind-lc-sses-2-L	colored	2	*Borassus*	Dr Jaengsawang	lek chan	Sesame oil + soot
ind-lc-slem-3-L	colored	3	*Borassus*	Dr Jaengsawang	lek chan	Lemongrass oil + soot
ind-lc-snem-4-L	colored	4	*Borassus*	Dr Jaengsawang	lek chan	Neem oil + soot
ind-lc-sric-5-L	colored	5	*Borassus*	Dr Jaengsawang	lek chan	Castor oil + soot
ind-lc-scit-6-L	colored	6	*Borassus*	Dr Jaengsawang	lek chan	Citronella oil + soot
ind-lc-seuc-7-L	colored	7	*Borassus*	Dr Jaengsawang	lek chan	Eucalyptus oil + soot

Synchrotron X-ray fluorescence mapping

Synchrotron X-ray fluorescence (XRF) mapping was performed on historical palm-leaf manuscripts and mock-ups during four beamtimes: three took place at the P62 beamline of PETRA III (DESY, Hamburg, Germany) [14–16], and one at the BM02 beamline of the European Synchrotron Radiation Facility (ESRF, Grenoble, France) [17]. Experimental parameters for each of the beamtimes are presented in Table 2, including sample number assigned, the orientation of

the object plane with respect to the beam (detailed sketch of the setup is published [10]), the beam energy and size on the sample, exposure time and the step size during the raster scan.

A table of measurements was built (Supplementary Data 1). The rows in the table are ordered according to *material type*: first manuscripts (historical objects) and then the mock-up samples, and are ordered in a secondary level alphabetically according to *object*, which is the identifier: shelf number in the case of the manuscripts and an assigned sample name in the case of the mock-ups. For each measurement the column *sample* indicates during which beamtime it was taken and hence the used parameters (see Table 2), as well as descriptive columns of the measurement area that indicate whether an area around a hole, edge, cracks or inscription (colored or not) is contained in the scan region. To later evaluate the composition at these areas, the pixels within the scan regions were categorized to the substrate, inscription, hole-adjacent, edge, or crack regions using masks constructed from the elemental maps and scan documentation as well as visual inspection of the maps. Pixels measuring air or the sample holder were also categorized as *None* and were not considered in the analysis. Fig. 1 shows an example of a scan region on a manuscript with the corresponding Ti and Fe maps, showing a higher intensity at the inscription and at the edge. Based on the image and the elemental maps pixels were assigned to different regions: substrate, inscription, edge or none. Panel (e) shows mean XRF spectra from substrate and inscription regions within the same measurement. Labels indicate the elemental line assigned to every peak.

Data analysis

Elemental differences between scan regions, including substrate, inscription, hole-adjacent, edge and crack regions, were evaluated from region-averaged XRF spectra. For each region, the spectrum was calculated as the mean of all pixels assigned to that region by the coordinate-defined masks. Elemental peak areas were obtained by direct integration after local background subtraction. For each characteristic line, a linear background was fitted from two sidebands, each 0.08 keV wide and separated from the integration interval by a 0.05 keV gap. The fitted background was subtracted and the residual signal was integrated within ± 0.08 keV of the nominal line energy.

The reproducibility and comparability of the extracted elemental profiles were assessed using pairwise root-mean-square (RMS) differences across the selected elements, without autoscaling. Within each beamtime, comparisons were performed between repeated measurements of the same folio, different folios of the same manuscript, and different manuscripts. Cross-beamtime comparability was evaluated by matching measurements from samples 0 and 3 according to manuscript identity and, where available, folio identity. Pairwise distances were aggregated at folio or manuscript level to prevent objects represented by multiple scans from receiving disproportionate weight.

The sensitivity of the resulting profiles to sample rotation was assesed as local surface geometry can modulate XRF intensities in incised objects [18]. Peak-integration window width, Compton normalisation, and standard- versus high-resolution acquisition was also evaluated. Several elemental representations were compared, including log-transformed peak areas, Compton-normalised intensities, centred log-ratio (CLR) coordinates [19], and inscription-to-substrate contrasts. Among the evaluated representations, conventional CLR coordinates provided the

Table 2: Experimental parameters at different beamtimes.

Beamline	Year	Sample number	α (°)	Energy (keV)	Beam (μm^2)	Exposure (s)	Step (μm)
P62	2024	0	$32, 45$	11.989	200	1	500 & 200
BM02	2024	$1, 2$	0	12.5	75	1	100
P62	2025	3	$0 - 50$	12.0	200	1	500
P62	2026	4	0	12.033	200	1	200

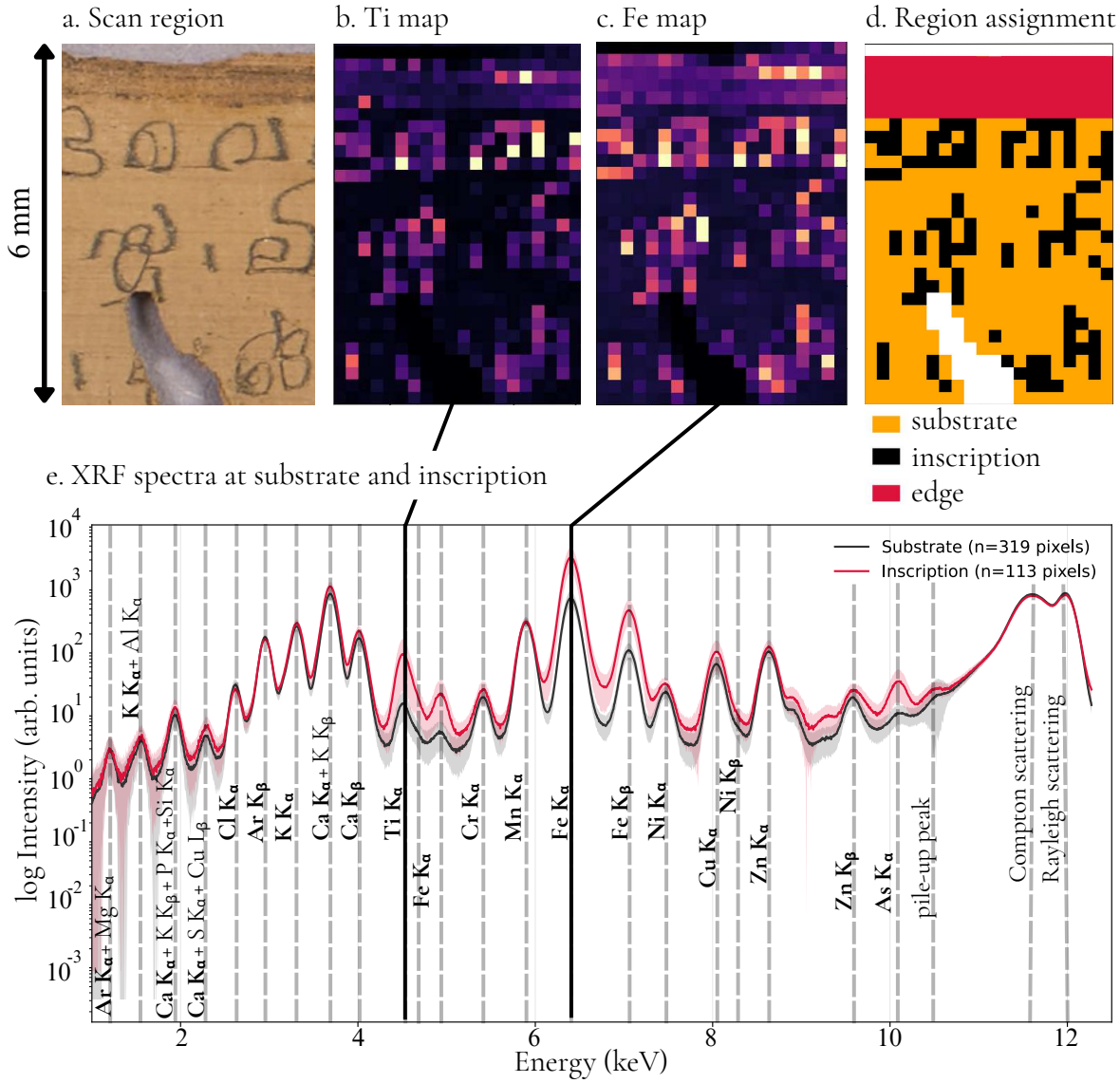


Figure 1: **Spatially resolved XRF analysis of object 2_2.** Sample 0, scan 46. (a) Approximate location of the scanned area. (b,c) Ti and Fe intensity maps, respectively; lighter colours indicate higher peak intensities. (d) Pixel assignments based on visual inspection and the elemental maps: substrate (orange), edge (red), and inscription (black). (e) XRF spectra averaged over the pixels assigned to the substrate (red) and inscription (black). Grey dashed lines mark the assigned elemental fluorescence lines. The most prominent differences between the spectra occur at the Ti and Fe lines. Shaded bands around the spectra indicate one standard deviation across the pixels assigned to each region.

most consistent comparability for standalone substrate and inscription profiles, while direct log ratios and ΔCLR were assessed for inscription-to-substrate contrasts. To accommodate differences in elemental peak availability across measurements, the subsequent comparative analysis employed a modified CLR transformation (mCLR) based on a fixed subset of reference elements, as defined below. The procedures, comparative results, and sensitivity analyses are reported in Supplementary Figures S1-S4. The analysis notebook and complete numerical outputs are provided in the accompanying data repository.

$$\mathrm{clr}(A_{r,e}) = \ln A_{r,e} - \frac{1}{E}\sum_{j=1}^{E} \ln A_{r,j}. \tag{1}$$

where $A_{r,e}$ is the locally background-corrected integrated peak area of element e in region r, E is the total number of elements included in the CLR transformation, and j is the index running over these elements. Thus, each elemental peak area is expressed relative to the geometric mean of the peak areas of all included elements.

As not all elemental lines yielded positive integrated areas in every region, a CLR transformation based on the complete elemental set could not be applied uniformly. For the consistency assessment, profiles were included only when all elements in the selected set had positive integrated areas. For subsequent comparisons among historical manuscripts, we therefore adopted a modified centred log-ratio transformation (mCLR), calculated relative to the geometric mean of a fixed reference set $\mathcal{B}$:

$$\mathrm{mclr}(A_{r,e}) = \ln A_{r,e} - \frac{1}{M}\sum_{j\in\mathcal{B}} \ln A_{r,j}, \tag{2}$$

here $\mathcal{B}$ comprised Al, Ca, Fe, K, Mn and Zn, and M is the number of elements, in this case 6. For elements belonging to $\mathcal{B}$, this quantity corresponds to a CLR coordinate calculated over the fixed reference set; for other elements, it represents a log contrast relative to that same reference.

Element-specific local enrichment was quantified as the direct log ratio between two regions,

$$\ln\left(\frac{A_{r_2,e}}{A_{r_1,e}}\right). \tag{3}$$

For the regional-enrichment barplots presented in the results, r_1 was the substrate and r_2 the region of interest within the same scan. Only standard-resolution measurements were included. For each manuscript and beamtime, the available log ratios were summarised separately for each region type and element by their median, with whiskers indicating the 25th–75th percentiles across measurements. These intervals describe the observed dispersion among measurements. Log ratios were calculated only when both integrated peak areas were finite and positive; unavailable values were omitted element by element without replacement.

Element-specific within-folio and between-folio variability references were calculated from measurements of the same region type. Absolute differences between log ratios were obtained for measurement pairs from the same folio or from different folios of the same manuscript. These differences were first summarised by their median within each folio or folio pair, respectively. The median of these summaries was then calculated across the available folio or folio-pair units within each beamtime, pooling manuscripts separately for each region type and element. References were displayed only when at least two valid units were available. Dashed and dotted markers were positioned at the manuscript-specific median contrast plus and minus the within-folio and between-folio references, respectively. These variability references were used to assess whether differences between region types could plausibly reflect variation among measurement locations. Differences between the median log ratios of two region types were compared with the typical differences observed between measurements of the same region type at different locations within a folio or on different folios of the same manuscript. Differences exceeding the corresponding

variability reference were interpreted as stronger descriptive evidence for a regional contrast. Because these references incorporate both spatial heterogeneity and measurement variability and were pooled across manuscripts, they were not treated as formal significance thresholds.

Comparative heatmaps used the corresponding difference in fixed-reference log contrasts,

$$\Delta\mathrm{mclr}_e = \mathrm{mclr}(A_{r_2,e}) - \mathrm{mclr}(A_{r_1,e}) \tag{4}$$

Positive direct log-ratio values indicate a higher signal in r_2 than in r_1. Positive or negative Δmclr values indicate that the elemental signal increases or decreases, respectively, relative to the geometric mean change of the reference elements between the two regions. They do not necessarily indicate an absolute increase or decrease in the integrated peak area.

Multivariate analysis was performed on inscription–substrate elemental $\Delta\mathrm{mclr}_e$, considering the fixed reference defined above. Only standard-resolution measurements were considered. For each object, the available inscription-substrate $\Delta\mathrm{mclr}_e$ were summarized as the element-wise median across measurements, so that each manuscript contributed one observation irrespective of the number of scans or folios measured.

Values were not imputed when an elemental contrast was unavailable. The primary PCA used the high-coverage elemental set Al, Ca, Cr, Cu, Fe, K, Mn, Ti, and Zn. Elements were included when finite object-level contrasts were available for at least 95% of the eligible manuscripts. This retained 25 of 26 eligible objects; one manuscript was excluded because Cr, Cu, and Ti were unavailable. The visibly red manuscript t12 was excluded before multivariate analysis, as well as the minoritary Thai group, containing only two manuscripts. Each elemental variable was autoscaled to zero mean and unit standard deviation across the retained objects before PCA, preventing variables with larger numerical dispersion from dominating the analysis [20]. PCA was fitted without country or species labels.

Country labels were subsequently overlaid on score plots for exploratory interpretation. India and Indonesia group centroids and 90% confidence ellipses were displayed in the score plots. To identify elemental directions aligned with the India–Indonesia contrast, loading vectors were projected onto the corresponding line joining the two group centroids; these projections were interpreted descriptively. Separation was additionally assessed in the full autoscaled nine-element space using a permutation test of the India–Indonesia centroid distance (9,999 permutations) and an omnibus PERMANOVA across countries [21]. A permutation test of multivariate dispersion (PERMDISP) was evaluated alongside PERMANOVA to assess possible differences in within-country dispersion [22].

Results

Elemental enrichment at historical inscriptions

XRF maps of the historical manuscripts frequently show localized elemental changes associated with the incised lines. Their elemental composition is not uniform across the dataset. Fe and Ti enrichment occurs in inscriptions from several objects, whereas Mn, Zn, Ni, Cu, and Cr make variable relative contributions in individual manuscripts. Fig. 2 provides an overview of inscriptional enrichment relative to the surrounding substrate, expressed using the defined Δmclr. Measurements were summarized at object level, except for three objects in which regions with and without blackening material within the incisions could be distinguished. These regions were summarized separately to assess whether their elemental patterns differ. In all three objects, the enrichment profiles were similar for blackened and unblackened regions, suggesting that the observed changes are primarily associated with the incision process itself, rather than with the blackening material.

Several manuscripts also exhibit As enrichment at the inscription relative to the surrounding support. This pattern is consistent with the possible application of arsenic-containing compounds

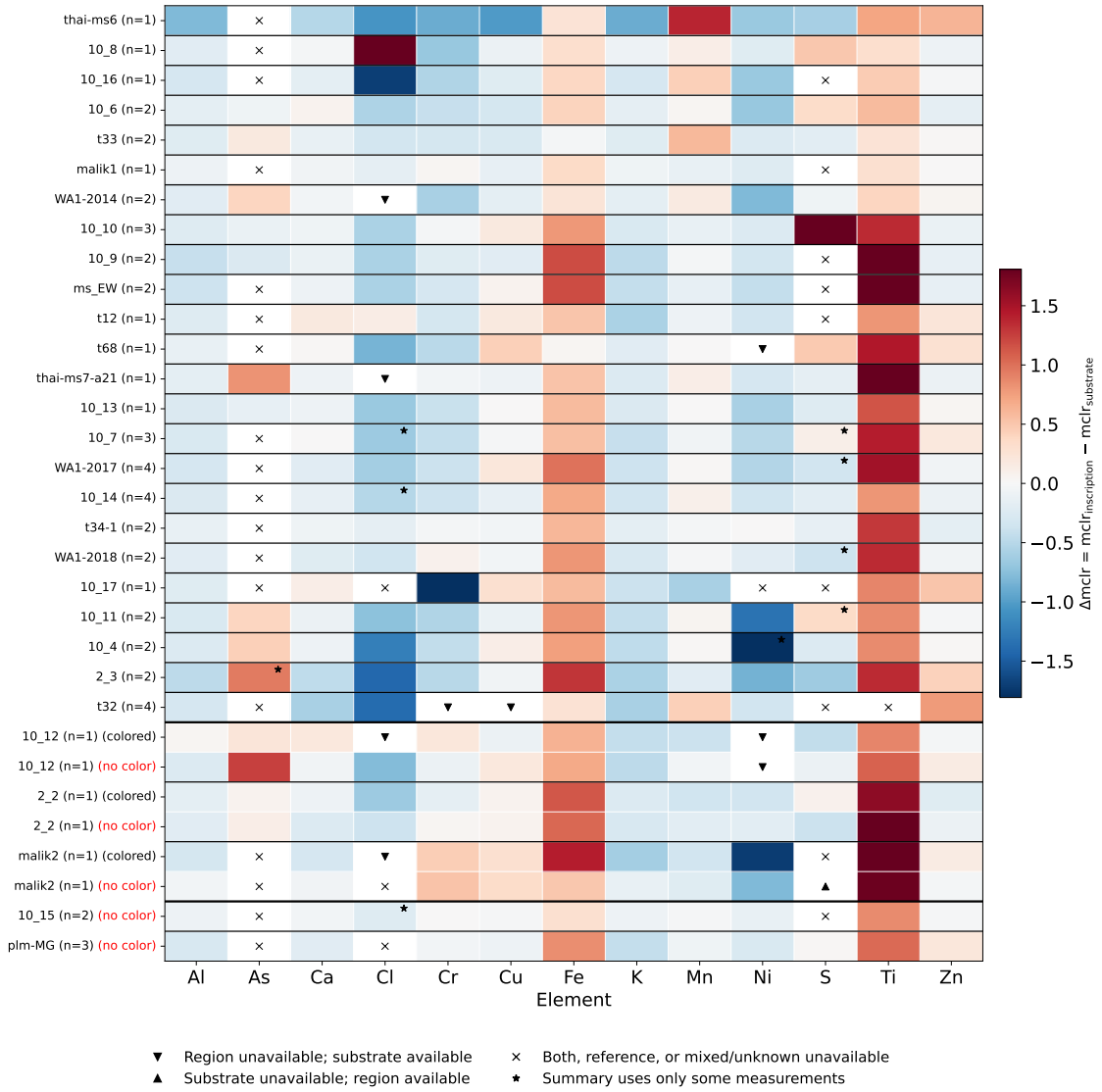


Figure 2: **Elemental contrasts at manuscript inscriptions.** Differences between inscription and substrate are expressed as Δmclr_e. Each square is coloured according to its value, from blue (most negative) through white (zero) to red (most positive). Measurements are summarized by manuscript object; the number in parentheses indicates the number of measurements contributing to the object-level summary. For manuscripts containing both blackened and unblackened incisions, these regions were summarized separately and are shown at the bottom. A cross indicates that no usable inscription–substrate contrast was available for that element. An asterisk indicates that the object-level median was calculated from only part of the available measurements. Downward and upward triangles indicate, respectively, that the peak area was unavailable in the inscription or in the associated substrate while remaining available in the other region.

reported in the literature [23]; however, its use cannot be confirmed from the XRF measurements alone.

Elevated intensities of metallic elements were also frequently observed around edges, cracks, and binding holes, often with elemental patterns distinct from those of the inscriptions. Fig. 3 illustrates this for one manuscript. The bar plot shows substrate-normalized logarithmic peak-area ratios for selected elements at the inscription, around a binding hole, and near an edge. The accompanying elemental maps show localized enrichment of Ca, Fe, Mn, and Ti at the inscription; Ca and Mn around the hole; and Ca, Mn, and Zn near the edge.

Edges and binding holes were produced using tools and may also retain blackening materials or preservation substances applied to the manuscript. Their elemental profiles nevertheless differ from those of the inscription and from each other. This observation indicates that no single, uniformly applied material can fully account for the observed enrichments. It is consistent with an additional contribution from the tools used to incise, perforate, or shape the leaves, although local differences in the retention of applied materials due to differences in local roughness may also contribute.

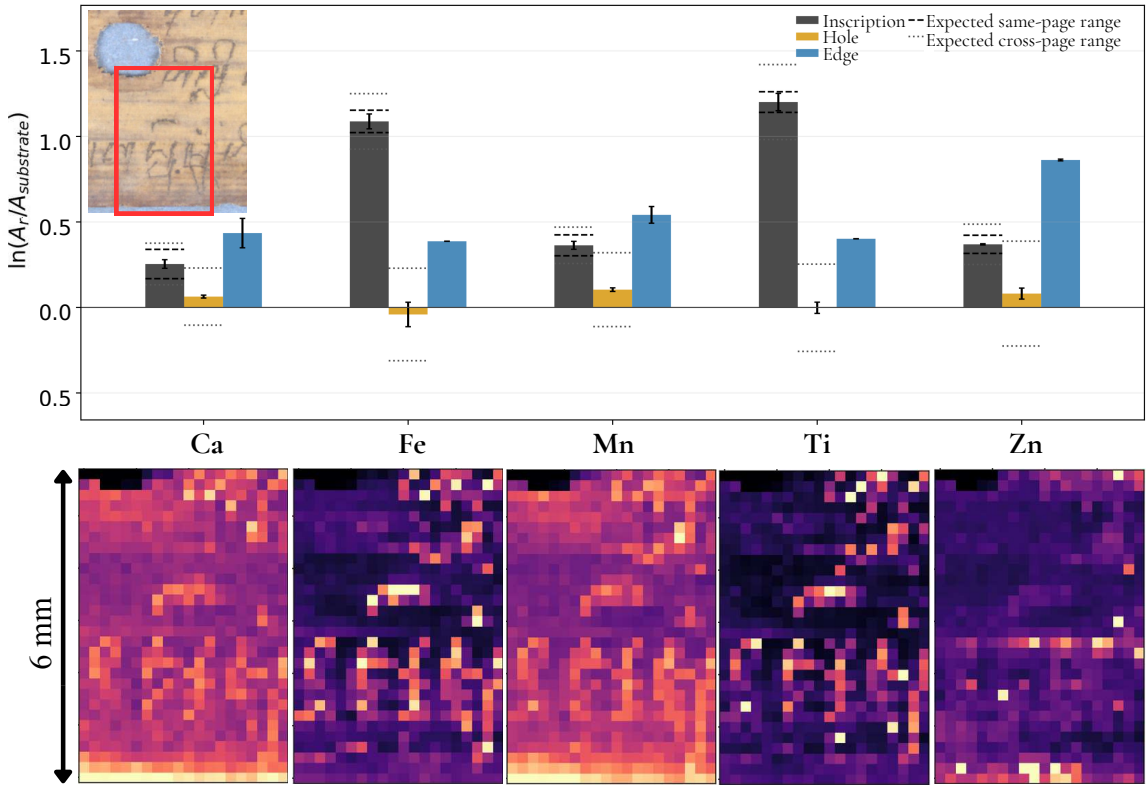


Figure 3: **Regional elemental contrasts in manuscript 10_4.** Logarithmic substrate-normalized peak-area ratios, $\ln(A_r/A_{\text{substrate}})$, for selected elemental fluorescence lines at an inscription (black bars), around a binding hole (yellow bars), and near an edge (blue bars). Bars show median log ratios across measurements; whiskers indicate the 25th–75th percentiles. Dashed and dotted horizontal markers indicate, where available, the median ± the typical within-folio and between-folio differences, respectively (see Methods for the calculation of bar summaries and variability references). The accompanying elemental maps show the spatial distributions of the elements discussed in the text. The red frame in the microscopy image shows the approximate measurement scan region.

The variation observed among manuscripts is consistent with diversity in manuscript manufacture and use, including the tools used to incise, cut, and perforate the leaves, as well as blackening and preservation materials applied during or after production [1, 2]. Substrate-

normalized elemental profiles for individual regions are provided as bar plots in the repository [24]. To compare features within the same object, feature–inscription contrasts were additionally summarized as heatmaps in the Supplementary Information.

The elemental origin of an enrichment cannot generally be assigned uniquely. A signal enhanced only at one type of feature—for example, at the edge but not at the hole or inscription—is consistent with a local contribution associated with that feature or its manufacture. Conversely, an element enriched at several feature types may originate from tool wear, applied materials, differential retention of those materials, or a combination of these processes. The results should therefore be interpreted as evidence of differing elemental histories of the features rather than as unambiguous identification of a particular tool or substance.

Cracks were present within the scanned area of only three manuscripts and measurements: 3,89 JAWI3_p3; 3,10 Malik1_letters; and 0,99 WA1-2018. In each case, the crack showed an elemental profile distinct from the surrounding substrate and broadly similar to that of the inscription. Although cracks can deepen or widen during deterioration, this similarity together with the dark color resembling that of the inscriptions, suggest that cracks may already have been present, or sufficiently open, when blackening material was applied. Alternatively, particulate material such as soot may have entered the cracks during the application of oils or other preservation media. Because cracks are not deliberately created with a writing tool, their similarity to the inscription does not provide a direct reference for stylus composition. Instead, it supports the interpretation that applied materials make an important contribution to the elemental enrichment observed at both features. Fig. 4 illustrates this pattern for WA1-2018.

Two manuscripts, 10_15 and plm-MG, showed no apparent blackening in any of the examined inscriptions or pages. Three further manuscripts: 2_2, 10_12, and malik2, contained pages or regions without apparent blackening. In these cases, a colouring medium may not have been applied locally, may have faded over time, or may have been removed during subsequent conservation or preservation treatments. Because some preservation oils are optically transparent, their presence at the inscription cannot be excluded. Nevertheless, these regions reduce one important source of compositional variation and are therefore particularly informative.

Manuscript 10_15, in which all examined pages appeared unblackened, demonstrates that an inscription-associated metal signal can persist even where no dark material is visible by optical microscopy. The binding hole showed enhanced Mn, Fe, Cu, Zn, and Ti signals (Fig. 5c). In contrast, the inscriptions on pages 4 and 7 contained no evident dark material within the grooves (Fig. 5a), yet the Fe maps reproduced parts of the incised lines (Fig. 5b). The other transition metals enhanced around the binding hole did not show comparably strong enrichment at these inscriptions. The measurement on page 7 additionally showed elevated Fe signal at the folio edge. Fig. 5d summarizes the substrate-normalized logarithmic enrichments for the inscription, hole, and edge regions.

Although a contribution from optically transparent preservation media cannot be excluded, the distinct elemental patterns at the edge, inscription, and hole are consistent with different histories of material deposition at these features. In particular, they are compatible with contributions from the different metallic tools used to cut, inscribe, and perforate the leaf, in addition to any subsequently applied materials.

Similar localized metal signals were observed in inscriptions with little or no visible blackening in manuscripts 10_12 and malik2. The corresponding micrographs, elemental maps, and regional-enrichment bar plots are provided in the Supplementary Information. Fig. 2 allows the Δmclr profiles of blackened and unblackened inscription regions within the same manuscript to be compared directly.

In manuscript 2_2, both blackened and unblackened inscriptions show pronounced Fe and Ti enrichment, consistent with a shared contribution associated with incision. The blackened region additionally shows a slight S enrichment, which may be related to the applied colouring material; its higher Fe signal may likewise reflect an Fe-containing component of that material. Manuscript

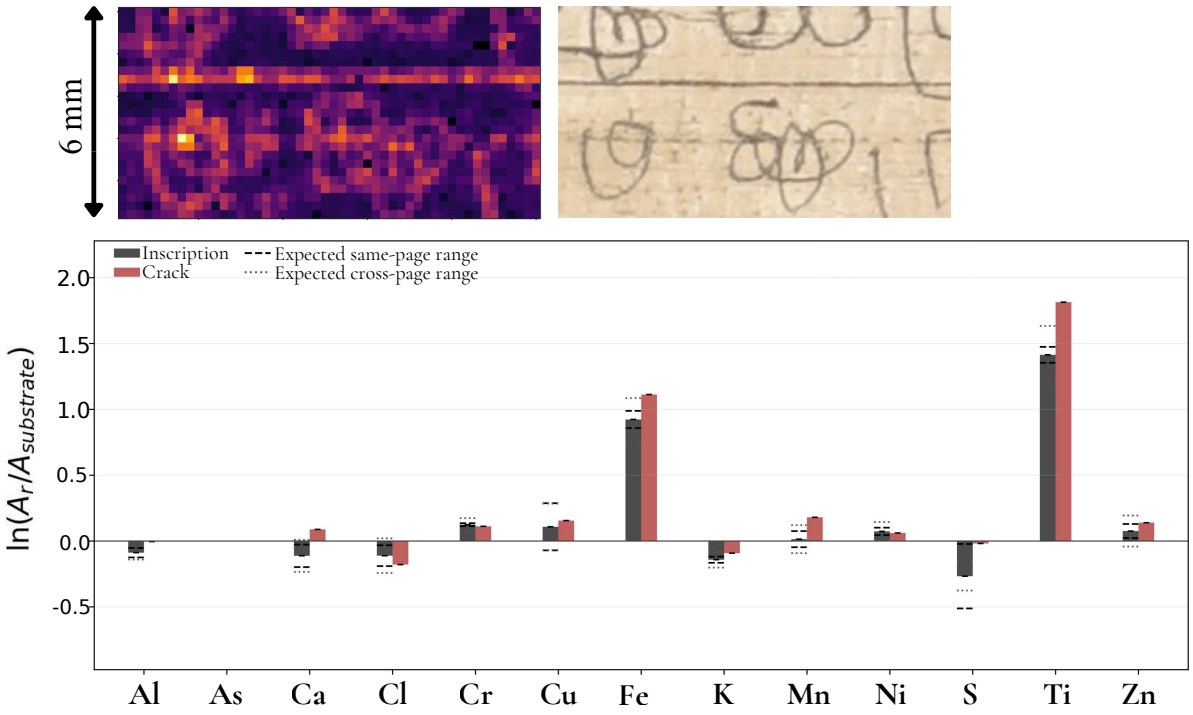


Figure 4: **Elemental contrasts at an inscription and a crack in manuscript WA1-2018.** Logarithmic substrate-normalized peak-area ratios, $\ln(A_r/A_{\text{substrate}})$, for selected elemental fluorescence lines at an inscription (black bars) and a crack (pink bars). Bars show median log ratios across measurements; whiskers indicate the 25th–75th percentiles. Dashed and dotted horizontal markers indicate the inscription median ± the typical within-folio and between-folio differences, respectively. No variability references are shown for cracks; these require at least two valid folio or folio-pair summaries (see Methods). The Fe intensity map shows enhanced signal both along the crack, visible as a horizontal feature across the scan area, and at the inscription. Their similar elemental profiles are consistent with a contribution from material deposited in both features, although the source and timing of this deposition cannot be established from XRF alone.

10_12 shows strong Fe and Ti enrichment in both region types, whereas the unblackened inscriptions have higher As, Cu, and Zn enrichment. Finally, manuscript malik2 shows prominent Cu, Fe, and Ti enrichment in both blackened and unblackened regions, with slightly higher Zn enrichment in the blackened region. These within-manuscript differences demonstrate that blackening material can modify the elemental pattern, but does not fully account for the enrichments observed at the incised lines.

The elemental signatures detected at inscriptions reflect both material transferred during incision and substances applied to the manuscript surface. These practices form part of manuscript manufacture and use traditions, which are known to vary substantially across South and Southeast Asia [2]. PCA was therefore used as an exploratory approach to assess whether broad geographical tendencies were present in the inscriptional elemental profiles.

PCA was performed on object-level median inscription Δmclr profiles. The nine elemental variables Al, Ca, Cr, Cu, Fe, K, Mn, Ti, and Zn were included because they were available for at least 95% of the eligible objects, retaining 25 manuscripts. Each variable was autoscaled before analysis to give all elements equal initial weight. Geographical origin was not used to fit the model, but was overlaid subsequently for interpretation.

The PC3 versus PC1 score plot showed the clearest, although still weak, geographical tendency (Fig. 6a). The groups overlap substantially rather than forming discrete origin clusters.

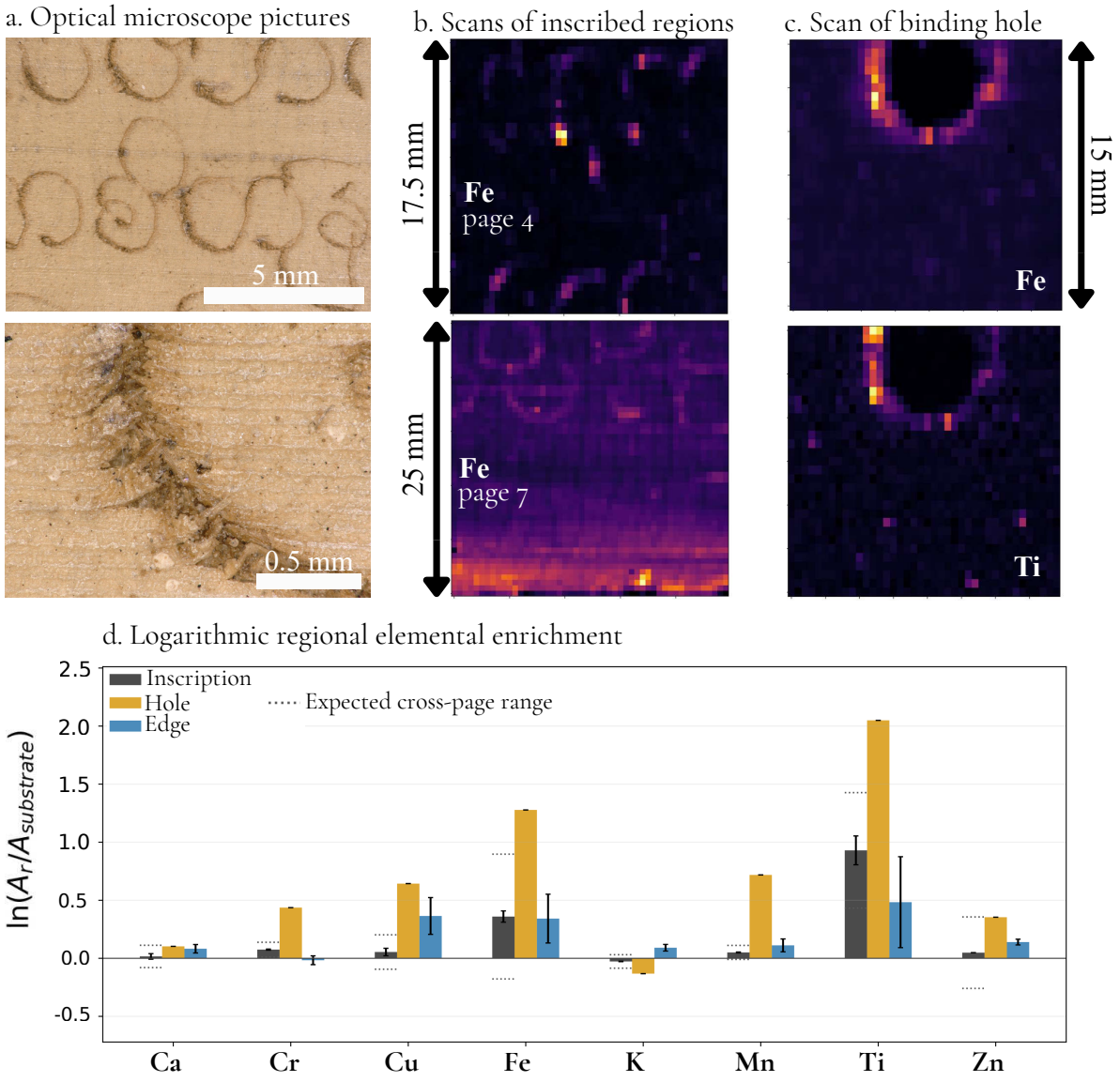


Figure 5: **Elemental characterization of manuscript 10_15.** (a) Optical micrographs of inscriptions without evident blackening material. (b) Fe maps of inscriptions on pages 4 and 7, showing localized Fe signals that follow parts of the incised lines. (c) Fe and Ti maps around a binding hole. (d) Logarithmic substrate-normalized peak-area ratios, $\ln(A_r/A_{\text{substrate}})$, for selected elemental fluorescence lines at inscriptions (black bars), around a binding hole (yellow bars), and near a folio edge (blue bars). Bars show median log ratios across measurements; whiskers indicate the 25th–75th percentiles for all region types. Variability references are shown only for inscriptions, as dotted horizontal markers at the median ± the typical between-folio difference (see Methods).

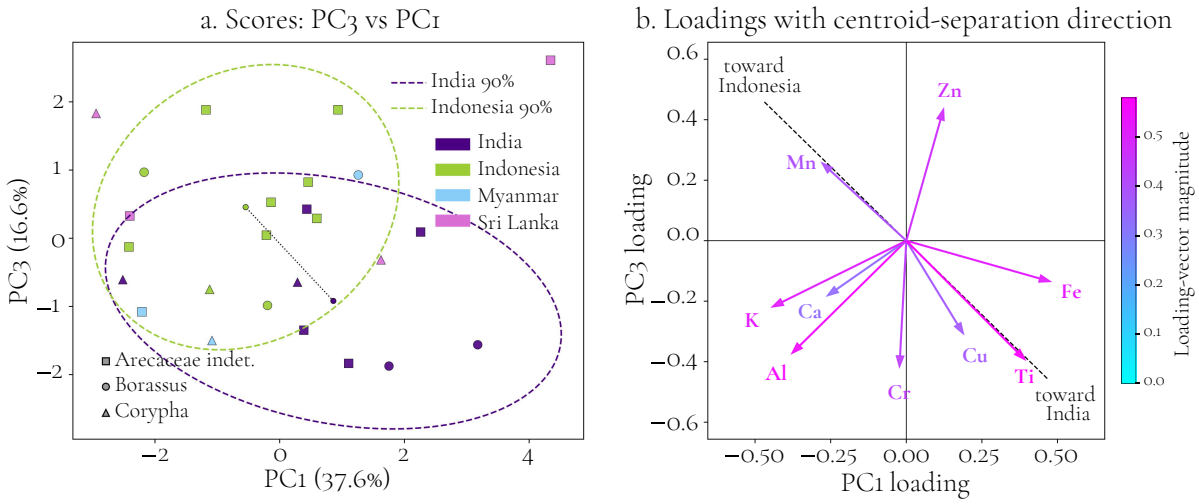


Figure 6: **Principal component analysis of inscription–substrate** Δmclr **profiles.** (a) Scores on PC1 and PC3. Colours indicate geographical origin: blue for India, green for Indonesia, light blue for Myanmar, pink for Sri Lanka. Marker shapes indicate the identified palm genera: squares for indetermined palm of the family Areacaceae, circle for *Borassus* and triangles for *Corypha*. Descriptive 90% covariance ellipses are shown for Indonesia and India. The dashed line connects their centroids, indicating the direction of separation between the group means in the displayed score plane. (b) Elemental loading vectors on PC1 and PC3. The dashed line indicates the centroid-separation direction from panel (a), providing a descriptive reference for interpreting the loadings in relation to the India–Indonesia contrast. The arrows are illustrated in a color scale ice blue to pink representing the module of the corresponding loading vector.

Nevertheless, the India and Indonesia groups show a partial shift in the PC1–PC3 plane. The Myanmar and Sri Lanka objects are more dispersed, but these groups contain few manuscripts and should therefore not be interpreted as defining robust regional patterns. Confidence ellipses are shown for India and Indonesia, the two groups with the largest number of objects. Their centroids are connected to indicate the direction of their separation in this score projection.

Fig. 6b shows the corresponding loading vectors. The dashed line represents the India–Indonesia centroid direction transferred to the loading plane and is used only as a descriptive guide. Mn lies approximately along the direction towards Indonesia, whereas Ti is aligned in the opposite direction, towards India. Cu and Fe form comparatively small angles with the Ti direction and are therefore also associated with the India side of this projected contrast, while Zn is more closely aligned with the Indonesia side. In contrast, K, Ca, and Al lie approximately perpendicular to the centroid direction and have little association with the India–Indonesia contrast in this PC1–PC3 projection. These patterns do not provide discrete geographical classification, but suggest weak regional tendencies in the relative elemental signatures of inscriptions that may reflect differences in local writing and preservation traditions. The broad overlap even between the majoritarian groups is likely due to the limited information offered by XRF, as different applied substances or tools may yield similar elemental signatures.

Experimental inscriptions

Experimental palm-leaf inscriptions were used to distinguish elemental signals potentially transferred during incision from those introduced during subsequent blackening and rubbing procedures. The measurements therefore included the traditional styluses themselves, unblackened incisions, and inscriptions treated with different blackening mixtures, see Table 1.

The two styluses used to prepare the mock-ups showed distinct XRF spectra. The Thai

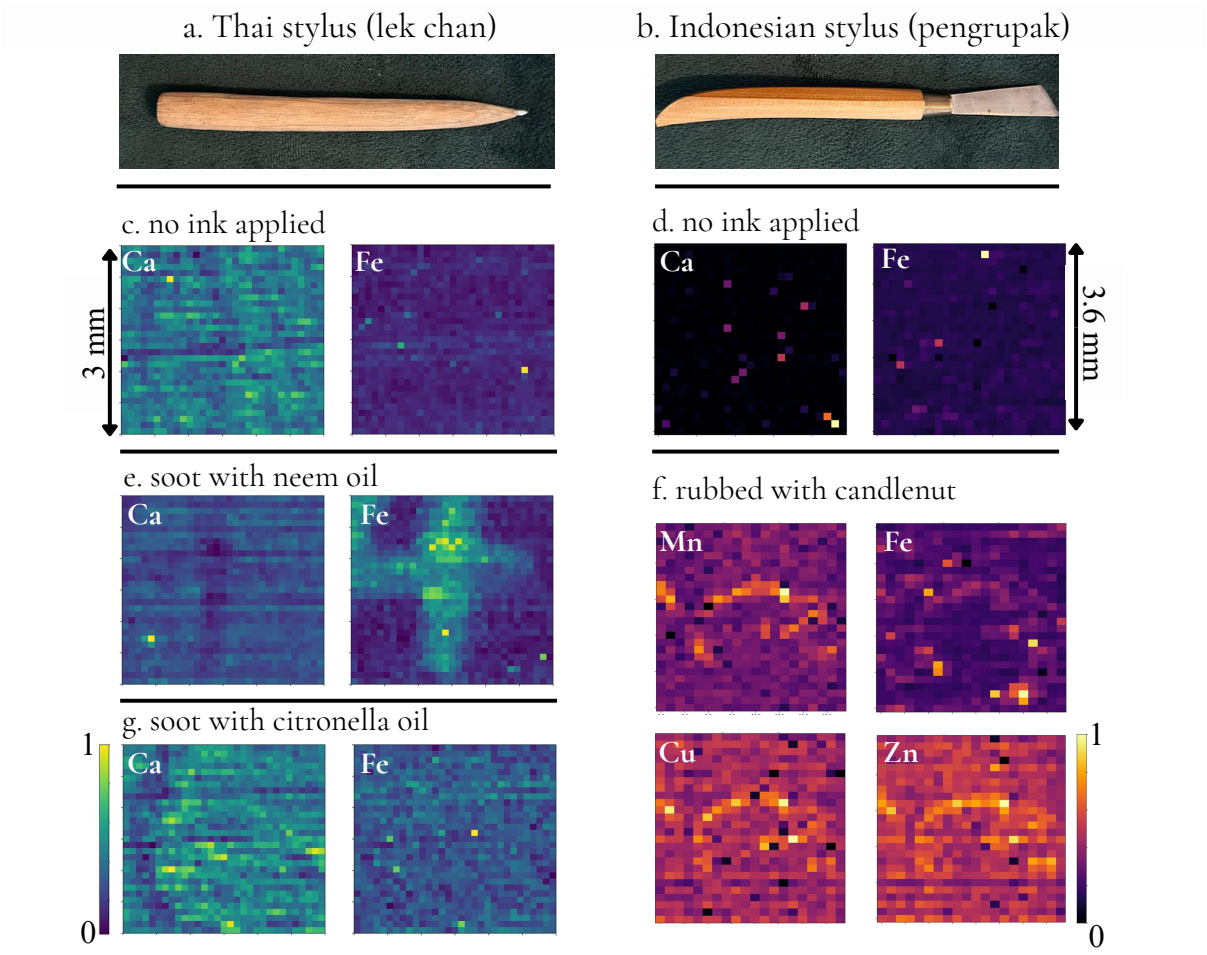


Figure 7: **Traditional styluses and elemental maps of experimental palm-leaf inscriptions**. (a) Thai *lek chān* stylus and selected elemental maps of mock-ups inscribed with this tool: (c) unblackened inscription area; (e) inscription treated with a soot–neem-oil mixture; and (g) inscription treated with a soot–citronella-oil mixture. (b) Indonesian *pengrupak* stylus and selected elemental maps of mock-ups inscribed with this tool: (d) unblackened inscription area and (f) inscription rubbed with burnt candlenut.

lek chān (Fig. 7a) produced a heterogeneous spectrum, with relatively Fe fluorescence and contributions from Ca, K, S, V, Ti, Mn, and Zn. In contrast, the Indonesian *pengrupak* (Fig. 7b) showed strong Fe fluorescence together with Mn, Cr, Ti, and Cl signals, see Supplementary Fig. 5. This pattern is consistent with an Fe-rich metallic tip, with additional signals potentially originating from its alloy composition or surface residues.

Despite the detectable elemental signals of the styluses, inscriptions made on modern palm-leaf supports and measured before blackening did not generally show strong localized metal enrichment (Fig. 7c,d). Under the tested conditions, the use of a metal-bearing stylus was therefore not sufficient to produce a consistently detectable elemental signature along the incised lines.

The application of blackening mixtures produced different outcomes depending on the preparation. Most soot–oil mixtures resulted in weak or indistinct elemental contrast at the inscription lines. In contrast, the soot–neem-oil mixture produced localized Fe enrichment following the incisions (Fig. 7e). On sample ind-pg-cn-text-P, rubbing with burnt candlenut produced enhanced Mn, Fe, Cu, and Zn signals at the inscriptions (Fig. 7f). These results show that metal-associated inscription patterns can arise during blackening and rubbing, even where

the initial incision did not show detectable elemental transfer from the stylus. No clear localized enrichment was observed after application of the soot–citronella-oil mixture (Fig. 7g).

Fig. 8 summarizes the substrate-normalized logarithmic enrichments for selected mock-ups made with the Thai stylus: inscriptions treated with soot–neem oil (top), soot–citronella oil (middle), and burnt candlenut (bottom).

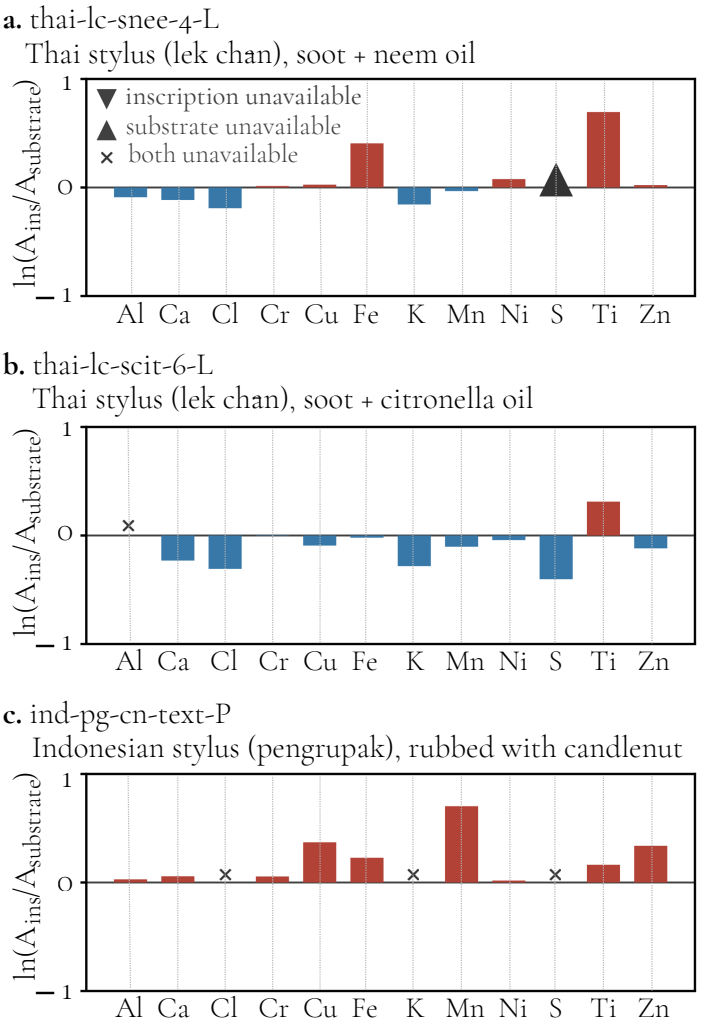


Figure 8: **Elemental contrasts in experimental inscriptions.** Substrate-normalized logarithmic peak-area ratios, $\ln(A_{\text{ins}}/A_{\text{substrate}})$, for selected experimental inscriptions made with the Thai stylus and treated with soot–neem oil (a), soot–citronella oil (b), and burnt candlenut (c). Here, ins denotes the inscription. Positive ratios (red bars) indicate higher peak areas at the inscription than in the substrate, whereas negative ratios (blue bars) indicate lower peak areas. Crosses mark unavailable ratios. When a usable peak area is unavailable in only one region, a downward-pointing triangle is used for unavailability at the inscription and an upward-pointing triangle for unavailability in the substrate.

Discussion

The combined measurements of historical manuscripts and experimental mock-ups show that elemental enrichment at palm-leaf inscriptions reflects a layered material history rather than a single source. Historical inscriptions frequently contained transition-metal enrichments, particularly Fe and Ti, but their elemental profiles varied considerably among objects and among different features of the same manuscript. Edges, binding holes, cracks, and inscriptions showed partially distinct enrichment patterns relative to their associated substrates. This feature-specific variation is difficult to explain by a single, uniformly applied blackening or preservation material alone. Instead, it supports contributions from the different tools involved in cutting, perforating, and inscribing the leaves, together with materials subsequently applied to their surfaces.

The measurements of apparently unblackened pages provide particularly informative evidence. In several cases, localized elemental enrichment remained detectable along incised lines despite the absence of visible dark material under optical microscopy. This observation is consistent with a contribution associated with the incision process itself. At the same time, the distinct elemental patterns observed at inscriptions, edges, and holes within individual manuscripts indicate that this contribution cannot be reduced to one common metal source. The similarity between some cracks and inscriptions further suggests that materials introduced during blackening or preservation may enter pre-existing cracks or other surface discontinuities. Thus, the elemental composition of an inscription may combine material transferred during manufacture with blackening compounds and later preservation media.

Previous analysis of Northern Thai palm-leaf manuscripts identified trace Fe in carbon-based writing material and considered both the soot paste and the metallic stylus as possible sources [8]. The mock-up experiments help assess these alternative contributions. They did not produce a consistently detectable elemental signature from stylus abrasion alone, even when traditional metal-bearing styluses were used. This result shows that metal transfer during incision is not inevitable and may depend on factors such as stylus condition, pressure, leaf properties, and the number of writing events. Modern styluses like the ones employed may be much harder and less prone to corrosion than older ones potentially used on some of the manuscripts evaluated in this work, thereby resulting in little to no material transfer. In contrast, particular traditional blackening and rubbing procedures generated localized Fe-rich or multi-element inscription patterns. The experiments therefore demonstrate that applied materials can make a substantial contribution to the elemental signatures observed at inscriptions.

Taken together, the results do not permit the unique assignment of an individual elemental signature to a particular stylus, blackening recipe, preservation treatment, or geographical tradition. They nevertheless establish that the elemental enrichment of palm-leaf inscriptions cannot be interpreted solely as evidence of stylus composition. Rather, it records the combined effects of writing, finishing, use, and preservation. This distinction is important for the interpretation of XRF measurements on historical manuscripts: variation between inscriptions may reflect differences in writing tools, but may equally reveal differences in the substances applied to make, maintain, or preserve the written surface. The inscription-focused analysis presented here complements our earlier investigation of structural and compositional signatures associated with botanical genus, manufacture, and provenance [10].

Data availability

The raw data of the synchrotron X-ray measurements at the ESRF are available in the ESRF data repository after the embargo period (April 2027) [17]. DESY datasets are listed at the DESY data repositories and available upon request [15, 16]. The DESY repositories also contain photos of the manuscript folios and the rough measurement area considered in each scan. Sample metadata and measurement information are provided in Supplementary Data 1 and 2. Additional

output of the analysis performed, including the applied masks, elemental maps, tables, and consistency checks are available in TORE [24].

Code availability

Custom Jupyter notebooks were used for data processing and analysis are available in TORE [24].

Author contributions

L.G. conceived the study, performed the experiments, carried out data analysis, and wrote the manuscript. M.B. contributed to the design of the experiments and setups, performed the experiments, assisted with data preprocessing. G.C. contributed to the assessment of manuscript origin based on codicological data and to the historical and manuscript-related interpretation. P.H. supervised the project and contributed to data interpretation. All authors reviewed and approved the final manuscript.

Competing interests

The authors declare no competing financial or non-financial interests.

Acknowledgements

The authors gratefully acknowledge the CSMC and its library, as well as the African Asian Institute (AAI) of the University of Hamburg, whose manuscripts are on permanent loan at the CSMC. We also thank the individuals who generously provided access to objects for measurement: Prof. Ewa Wilden, Prof. Volker Grabowsky, Prof. Jörg Fromm, Dr. Chieng Li, Alex Malik, and Malgorzata Grzelec. We also thank Giuseppe Marotta for his assistance during XRF measurements of the styluses.

We thank the synchrotron facilities that granted beamtime for this research, the European Synchrotron Radiation Facility (ESRF) and Deutsches Elektronen-Synchrotron (DESY), as well as the beamlines BM02 and P62. We are grateful to the beamline scientists Dr. Isabelle Morfin and Dr. Gilbert Chachine (ESRF) and Dr. Sylvio Haas (DESY) for their support during the experiments.

Funding

L.G. received support from the Deutsche Forschungsgemeinschaft (DFG) through the Excellence Strategy of the Federal Government and the federal states under EXC 2176/2 “Understanding Written Artefacts” (UWA).

References

1. Wiland, J. *et al.* A literature review of palm leaf manuscript conservation—Part 1: A historic overview, leaf preparation, materials and media, palm leaf manuscripts at the British Library and the common types of damage. *Journal of the Institute of Conservation* **45,** 236–259 (2022).
2. Agrawal, O. P. *Conservation of Manuscripts and Paintings of South-East Asia* (Butterworths, London, 1984).

3. Yani, Z. *et al.* Traditional Ways of Caring for Historical Manuscripts in Lombok (Indonesia). *Restaurator. International Journal for the Preservation of Library and Archival Material* **46,** 171–183 (2025).
4. Sharma, D., Singh, M. R. & Dighe, B. Chromatographic study on traditional natural preservatives used for palm leaf manuscripts in India. *Restaurator. International Journal for the Preservation of Library and Archival Material* **39,** 249–264 (2018).
5. Wiland, J. *et al.* A literature review of palm leaf manuscript conservation—Part 2: historic and current conservation treatments, boxing and storage, religious and ethical issues, recommendations for best practice. *Journal of the Institute of Conservation* **46,** 64–91 (2023).
6. Yu, D. *et al.* The Effect of Traditional Processing Craft on the Hygroscopicity of Palm Leaf Manuscripts. *Heritage Science* **12,** 280 (2024).
7. Yu, C., Zhang, M., Li, B. & Lian, X.-D. Unraveling the Ink Composition of Ancient Palm Leaf Manuscript from Tibet: A Multi-Analytical Study. *npj Heritage Science* **13,** 73 (2025).
8. Sathiyamani, S. *et al.* Material Characterisation of 19-20th Century Manuscripts from Northern Thailand. *Restaurator* (2024).
9. Singh, M. R. & Sharma, D. Investigation of Pigments on an Indian Palm Leaf Manuscript (18th-19th century) by SEM-EDX and other Techniques. *Restaurator* **41,** 49–65 (2020).
10. Gallardo, L., Busch, M., Poliakova, A., Ciotto, G. & Huber, P. Multimodal synchrotron X-ray analysis of palm-leaf manuscripts: structural and compositional signatures of botanical genus, manufacture, and provenance. *npj Heritage Science* **14,** 527 (2026).
11. Nehring, G., Gordon, N. & Rabin, I. Distinguishing between seemingly identical inks using scanning μXRF and heat maps. *Journal of Cultural Heritage* **57,** 142–148 (2022).
12. Zerbe, K., Gallardo, L., Cameli Manzo, R., Haas, S. & Hammel, J. U. Synchrotron Radiation for Cultural Heritage at PETRA: From Micro- and Nanoscale Spectro-Microscopy to 3D Imaging at PETRA III—with a View to PETRA IV. *Synchrotron Radiation News.* Published online 22 October 2026, 1–7 (2026).
13. Rachman, Y. B. Palm Leaf Manuscripts from Royal Surakarta, Indonesia: Deterioration Phenomena and Care Practices. *Restaurator. International Journal for the Preservation of Library and Archival Material* **39,** 235–247 (2018).
14. Haas, S., Sun, X., Conceição, A. L. C., Horbach, J. & Pfeffer, S. The new small-angle X-ray scattering beamline for materials research at PETRA III: SAXSMAT beamline P62. *Journal of Synchrotron Radiation* **30,** 1156–1167 (2023).
15. Huber, P. *Palm leaves as writing support: Compositional and multiscale structural analysis to trace the history of Asian manuscripts* (DESY, 2026).
16. Huber, P. *Understanding the production of palm leaf manuscripts: additional measurements for data completeness* (DESY, 2026).
17. Gallardo Dominguez, L. & Busch, M. *Palm leaves as writing support: compositional and multiscale structural analysis to trace the history of Asian manuscripts* Dataset, European Synchrotron Radiation Facility. 2027.
18. Geil, E. C. & Thorne, R. E. Correcting for surface topography in X-ray fluorescence imaging. *Journal of Synchrotron Radiation* **21,** 1358–1363 (2014).
19. Aitchison, J. Principal component analysis of compositional data. *Biometrika* **70,** 57–65 (1983).
20. Jolliffe, I. T. & Cadima, J. Principal component analysis: a review and recent developments. *Philosophical Transactions of the Royal Society A: Mathematical, Physical and Engineering Sciences* **374,** 20150202 (2016).

21. Anderson, M. J. A new method for non-parametric multivariate analysis of variance. *Austral Ecology* **26,** 32–46 (2001).

22. Anderson, M. J. Distance-Based Tests for Homogeneity of Multivariate Dispersions. *Biometrics* **62,** 245–253 (2006).

23. Delhey, M., Kindzorra, E., Hahn, O. & Rabin, I. Material analysis of sanskrit palm-leaf manuscripts preserved in Nepal. *Journal of the international association of buddhist studies,* 119–152 (2013).

24. Gallardo, L., Busch, M. & Huber, P. *Analysis of elemental signatures at palm-leaf manuscripts inscriptions* (TORE, 2026).

Supplementary Files

This is a list of supplementary files associated with this preprint. Click to download.

- SupplementaryData1.xlsx
- SI.pdf